



<b>Experiment title:</b> X-ray diffraction study of amorphous and crystalline GeSe <sub>2</sub> at high pressures and temperatures	<b>Experiment number:</b> HS1228
<b>Beamline:</b> ID30	<b>Date of experiment:</b> from: 11/05/00                      to: 17/05/00
<b>Shifts:</b> 15	<b>Local contact(s):</b> M. Mezouar & W. A. Crichton
<b>Date of report:</b> 27/02/01  <i>Received at ESRF:</i>	

**Names and affiliations of applicants (\* indicates experimentalists):**

Tor Grande<sup>1\*</sup>, Svein Stølen<sup>2\*</sup>, Andrzej Grzechnik<sup>3\*</sup>, Wilson Crichton<sup>4\*</sup> & Mohamed Mezouar<sup>4\*</sup>

<sup>1</sup> Norwegian University of Science and Technology, Trondheim. <sup>2</sup> University of Oslo, Oslo.

<sup>3</sup> MPI für Festkörperforschung, Stuttgart. <sup>4</sup> ESRF.

**Report:**

Herein we report information both on the existence of distinct GeSe<sub>2</sub> crystalline and liquid modifications with different connectivity schemes and on the phase diagram of this material in the pressure range up to about 6 GPa as determined by *in situ* synchrotron angle-dispersive x-ray powder diffraction, Figure 1. In general, crystal chemistry investigations of chalcogenide Ge and Si systems at different pressure and temperature conditions are important to better understand the structural framework in the corresponding amorphous materials. At elevated pressures, four-to-six coordination changes around the cations and/or changes in dimensionality of the structures are expected in the crystalline phases. Similar structural transformations could be envisioned in related melts and glasses, with a possibility of synthesizing different amorphous polymorphs.

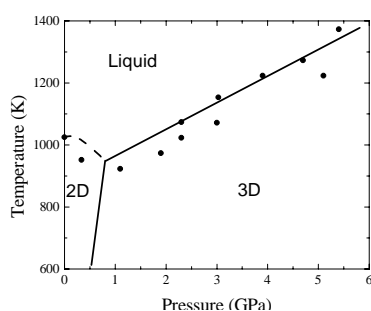


*Figure 1 Phase diagram and melting curve of GeSe<sub>2</sub>*

Upon decreasing the interlayer separation, i.e., upon compression, the 2-D  $P2_1/c$  monoclinic phase of GeSe<sub>2</sub> becomes unstable and pressure-induced amorphization is observed at 11-14 GPa at room temperature<sup>1</sup>. On the other hand, on temperature increase, i.e., upon isobaric heating, monoclinic GeSe<sub>2</sub> melts. At atmospheric pressure, melting of this phase occurs at 1025 K. When two-dimensional GeSe<sub>2</sub> is compressed at the pressure range up to 6 GPa at temperatures 600-1400 K, only one new crystalline modification, along with its distorted variants, is observed. The x-ray patterns collected at the temperature range 600-700 K have admixtures of both polymorphs, indicating a presence of kinetics effects associated with this transformation. We already determined the new structure using direct methods for x-ray powder diffraction and a full profile Rietveld refinement method. This three-dimensional GeSe<sub>2</sub> polymorph has  $I\bar{4}2d$  ( $Z = 4$ ) space group. The Ge and Se atoms are at the  $4a$  (0,0,0) and  $8d$  ( $x,0.25,0.125$ ) Wyckoff sites, respectively<sup>2</sup>. The structural variations and different distorted variants at lower symmetries ( $P-4$ ,  $I-4$ )<sup>3</sup>, depending on the actual pressure and temperature conditions, can be explained by anisotropic lattice distortions due to cooperative tiltings of the rigid GeSe<sub>4</sub> units, i.e., through an angular deformation of the Ge<sub>4</sub>Se<sub>10</sub> unit consisting of four corner-sharing tetrahedra. First-coordination interatomic distances in this polymorph are comparable to those in the two-dimensional structure<sup>4</sup>.

In this context, our experimental results on the crystalline polymorphs presented here are also considered as a basis for structural analysis of GeSe<sub>2</sub> liquids generated at high pressures and high temperatures, where the data were again obtained during *in situ* investigation. GeSe<sub>2</sub> has in fact been shown to *tend* towards a more metallic structure in ambient pressure neutron studies<sup>5</sup>. Yet, to our knowledge there has been no previous high-pressure study of liquid GeSe<sub>2</sub>.

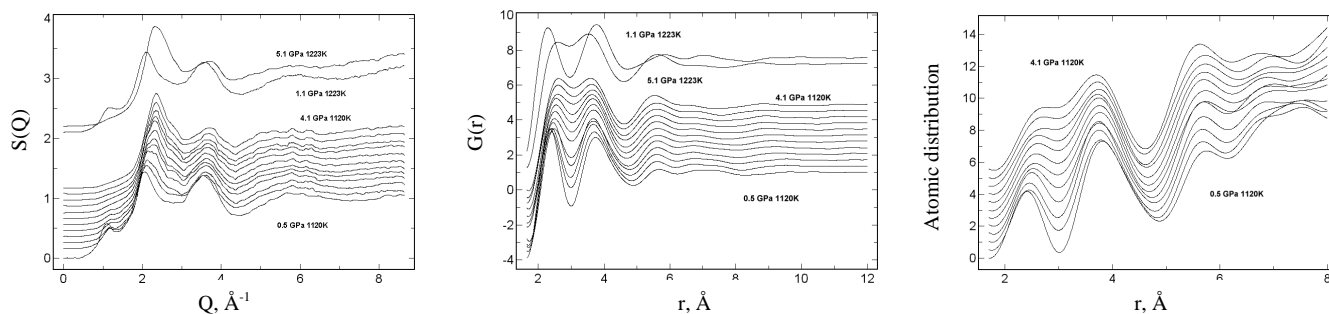


Figure 2. a)  $S(Q)$  obtained directly from background subtraction and normalisation of diffraction data. b) The  $G(r)$  for the same data, by Fourier transform and c) the  $4\pi r^2\rho G(r)$  atomic distribution curve from which coordination numbers are obtained through use of the EoS of Stølen et al<sup>7</sup> and the densities and thermal expansivities of Ruska and Thurn<sup>8</sup>.

The  $S(Q)$ s show features widely associated with  $\text{GeSe}_2$  glasses and liquids in that they have, at low pressure, the first sharp diffraction peak (FSDP) at  $\sim 0.9\text{\AA}^{-1}$  indicative of periodicity of  $\text{GeSe}_4$  tetrahedra in the 2D array through correlation of Ge-Ge interactions<sup>6</sup>, Figure 2a. At higher  $Q$ , the peaks associated with the Ge-Se and Se-Se, Ge-Ge interactions are seen prominently at  $\sim 2.1\text{\AA}^{-1}$  and  $\sim 3.6\text{\AA}^{-1}$ . There is clear reduction in the FSDP with increasing pressure, indicating a changing conformation of tetrahedral coordinated species. There is almost complete diminution of the FSDP above  $\sim 2.5\text{GPa}$ . If we study the peak positions and widths in  $S(Q)$  we see a 5% discontinuous shift in position at  $2.30\text{GPa}$ . Peak broadening increases through the first 4 data until at maximum at  $2.10\text{GPa}$  it reaches  $0.85(3)\text{\AA}^{-1}$ , compared to initial at  $0.55(2)\text{\AA}^{-1}$  and minimum at  $0.43(2)\text{\AA}^{-1}$ ,  $3.87\text{GPa}$ . These are linked to the asymmetry in the Ge-Se peak, which originates from the presence of a range in Ge-Se and Ge-Ge distances and asymmetry increases due to the difference in local compressibilities of the Ge-Ge and Ge-Se regions. Onset of the change in connectivity can be seen quite clearly in both asymmetry and peak position shift, marking a change in Ge-Se bonds that reflects a lower range in population (higher local symmetry; e.g.  $P2_1/c$  has 4 symmetrically independent Ge sites thus many more Ge-Se bonds, whereas  $I4_2d$  has only one unique Ge position and one Ge-Se bond) and different average bond Ge-Se bond length. The  $G(r)$ , obtained by Fourier transform of the  $S(Q)$  appears much smoother due to the rejection of irregularities in the frequency domain, shows similar features to the  $S(Q)$  curves, Figure 2b. The most prominent feature, not immediately obvious from the diffraction data is the increase of intensity at the minimum at  $\sim 3\text{\AA}$ , other salient points are the merging of peaks at around  $7\text{\AA}$  and  $9\text{\AA}$  and the increase of intensity and sharpening of the Se-Se peak at  $5.5\text{\AA}$ , again indicating a lower range in Se-Se distances from increase in local symmetry. By comparison of the discontinuities seen in the  $S(Q)$  with those of the  $G(r)$  we find the response to transition in the  $G(r)$  varies with  $r$ . It is clear from the atomic distribution curves that there are no substantial changes in CN about the first two peak positions, but is however increasing in the third; indicating that the polymeric unit is larger than the tetrahedra in size, Figure 2c.

We have obtained information that the intermediate-range neighbourhood conformation has changed, by changing peak intensities, merging of next-nearest neighbour peaks (e.g. at  $7\text{\AA}$ ) and discontinuities at high- $r$ . The transformation is seen to start at an increasing pressure as we go to higher neighbour distances, which is taken as proof that the structure can accommodate structural transition at different levels and that there is more than one order parameter involved in the transition. This gives rise to the intermediate region (which is only  $0.3\text{GPa}$  wide) that is predicted as a feature of general liquid-liquid transition. We infer from the phase diagram that there is no appreciable density difference between the liquid phases produced. From these, we interpret the change in the liquid as a polymerisation, increasing local symmetry from locally monoclinic based  $\sim 4:2$  liquid to one based on the  $4:2$  coordinated tetrahedral  $\text{GeSe}_2$  and  $\text{GeS}_2$  phases, increasing dimensionality from 2D chains to a 3D network.

## References.

1. A. Grzechnik, T. Grande, S. Stølen (1998) *J. Solid State Chem.* **141**, 248
2. T. Grande, M. Ishii, M. Akaishi, S. Aasland, H. Fjellvåg, S. Stølen (1999) *J. Solid State Chem.* **145**, 167
3. A. Grzechnik, S. Stølen, E. Bakken, T. Grande, M. Mezouar (2000) *J. Solid State Chem.* **150**, 121
4. G. Von Dittmar, H. Schaffer (1976) *Acta. Cryst. B* **32**, 2726
5. P. S. Salmon, I. Petri, W. S. Howells (1999) ISIS Rutherford Appleton Laboratory Report #10260
6. P. S. Salmon, J. Liu (1994) *J. Phys.: Cond. Matter* **6**, 1449
7. S. Stølen, A. Grzechnik, T. Grande, M. Mezouar (2000) *Solid State Comms.* **115**, 249
8. J. Ruska, H. Thurn (1976) *J. Non-Cryst. Solids* **22**, 277